Nanoscale Dislocation Patterning in PbTe/PbSe(001) Lattice-Mismatched Heteroepitaxy

G. Springholz and K. Wiesauer

Institut für Halbleiter- und Festkörperphysik, Johannes Kepler Universität, A-4040 Linz, Austria

(Received 26 April 2001; published 19 December 2001)

Dislocation patterning in PbTe on PbSe (001) heteroepitaxy is studied using scanning tunneling microscopy. It is shown that exceedingly regular square arrays of misfit dislocations are formed during strain relaxation. This is based on the existence of a homogeneous dislocation nucleation process, a high dislocation mobility within the interface, and an effective repulsive interaction between neighboring dislocations. Similar results are expected also for other highly mismatched heteroepitaxial systems.

DOI: 10.1103/PhysRevLett.88.015507 PACS numbers: 81.16.Rf, 61.72.Ff, 68.37.Ef, 68.55.Jk

Pattern formation during lattice-mismatched heteroepitaxy has recently evolved as a novel tool for self-assembled fabrication of low-dimensional semiconductor nanostructures [1]. An example is the direct synthesis of quantum dots via the Stranski-Krastanow growth mode [2] where nanometer-size coherent islands spontaneously nucleate on the surface of a wetting layer. Usually, however, these islands exhibit a broad size dispersion and nucleate at random positions on the epitaxial surface. As shown by recent work [3–6], this situation can be improved by dislocation prepatterning of the structures due to the spatial control of the dot nucleation sites by the localized strain fields of subsurface misfit dislocations. As a result, a linear alignment of the dots in patterns of chains above misfit dislocations has been obtained [3–5]. In semiconductor heterostructures, however, misfit dislocations are usually distributed in a highly *irregular* way within the layers [7,8]. This is because the dislocations are usually generated from extrinsic nucleation or multiplication sources [7], and because the dislocation glide planes are usually *inclined* to the heterointerfaces. As a result, the dislocations are rather immobile within the interface, and, therefore, their lateral arrangement is mostly determined by the irregular distribution of nucleation sources.

In this Letter, it is shown that highly periodic dislocation patterns can be produced if several conditions are fulfilled. These are (i) a high dislocation mobility within the interface, (ii) the existence of a homogeneous nucleation mechanism, and (iii) a strong repulsive dislocation interaction. As shown in this work, these conditions are met for the PbTe/PbSe (001) heteroepitaxial system. From detailed scanning tunneling microscopy (STM) investigations, we find that, in spite of the large -5.2% lattice mismatch, a 2D growth mode prevails during growth. Therefore, strain relaxation occurs purely by misfit dislocation formation. These dislocations are of pure edge character, and their Burgers vector is oriented parallel to the interface. Because of the resulting high mobility, a nearly perfect square array of edge dislocations is formed with a lateral period of 10–20 nm. The regularity of this pattern scales inversely with dislocation spacing that crucially determines the strength of the dislocation interactions. Thus, for the smallest separations, a dispersion in dislocation spacings of less than $\pm 12\%$ is achieved, a value that is significantly better than those typically attained for self-assembled Stranski-Krastanow dots.

The samples were grown by molecular beam epitaxy using PbTe and PbSe as beam flux sources. Both compounds crystallize in the rock salt structure with lattice constants of 6.462 and 6.124 Å, respectively. Onto chemomechanically polished (001) oriented PbSe substrates, first, several μm thick PbSe buffer layers were deposited at a temperature of 380 °C. Then, PbTe or PbSeTe ternary layers were grown on top with thicknesses varying from 1–20 monolayers (ML), where 1 ML corresponds to 3.23 Å layer thickness. The deposition rate was 0.4 ML/s and the substrate temperature was 380 °C. After growth, the samples were immediately cooled to room temperature and transferred under ultrahigh vacuum conditions to a separate chamber for STM imaging of the epitaxial surface structure. STM images were acquired at a sample bias of 0.4–1 V and a tunneling current of 0.4–1 nA.

Figure 1 shows a series of STM images of layers at thicknesses of 0.3, 4.5, and 9 monolayers. In striking contrast to the (111) growth orientation [9], growth proceeds in a 2D step flow growth mode without Stranski-Krastanow island formation. This is due to the fact that the nonpolar (001) surface is the lowest free energy surface of PbTe [10]. Therefore, the additional surface energy for island formation is large compared to the energy that can be gained from elastic relaxation within the islands. At coverages below 1 ML [Fig. 1(a)], the PbTe surface terraces are featureless flat similar to those of the initial PbSe substrate surface. At higher coverages, however, [Figs. 1(b) and 1(c)], a high density of dark lines appears superimposed in the STM images. As indicated in the magnified STM image of Fig. 1(d), these dark lines are all aligned along the $\langle 110 \rangle$ surface directions and correspond to a local surface depression of about 0.4 Å, and of 0.8 Å at each line crossing. These depressions are caused by the local lattice distortions around subsurface misfit dislocations (see Refs. [11–13]) formed when the layer exceeds the critical thickness. Thus, each dark line signifies the presence of a misfit dislocation at the heterointerface.

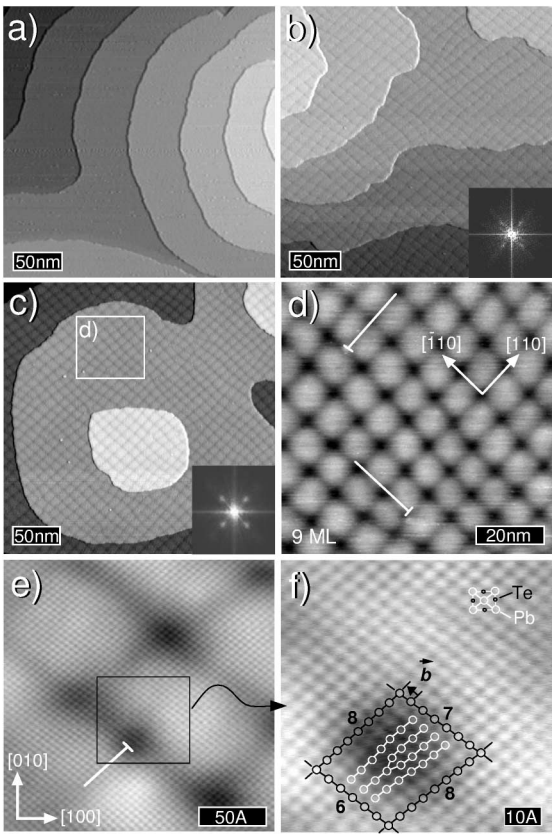

FIG. 1. STM images of PbTe epilayers on PbSe (001) at coverages of 0.3 ML (a), 4.5 ML (b), and 9 ML (c)–(f). The dark lines are caused by subsurface misfit dislocations. Insets in (b) and (c): Fourier transform power spectra of the STM images. The dislocation configuration is derived from the atomically resolved STM images (e) and (f), where the corresponding Burgers circuit is drawn around one of the threading dislocations.

Direct evidence for this correlation comes from atomically resolved STM images of the end points of the dark lines. Because every dislocation must be terminated at a free crystal surface, there are two threading dislocations that connect each misfit dislocation with the layer surface. The empty-state STM image of one of these threadings is shown in Fig. 1(f). From the Burgers circuit along the atomic rows around the dislocation core, one immediately sees that a Burgers vector of $\vec{b} = (1/2)[\bar{1}10]$ is required to close the circuit. This vector is parallel to the interface and perpendicular to the dislocation line direction. Thus, each dislocation corresponds to a vertical $(\bar{1}10)$ lattice half-plane removed from the crystal to accommodate the layer/substrate mismatch. Such dislocations cannot be formed by glide but only by vertical climb through removal of atoms by absorption of vacancies or by emission of atoms to the free layer surface. This is consistent with the fact that no glide steps are observed on the surface [12,13]. The given orientation of $\vec{b}$ also explains the dislocation alignment along the $\langle 110 \rangle$ directions because this orientation maximizes the strain relaxed by each dislocation.

Certainly the most striking feature of the STM images is the remarkable uniformity of the dislocation arrangement, forming a quasiperiodic grid with a line spacing of only about 10 nm [14]. This is clearly evidenced by the appearance of fourfold symmetric satellite peaks in the Fourier transform power spectra of the STM images shown as insets in Fig. 1. The satellite positions are inversely proportional to the average dislocation spacing $\langle L \rangle$ that is plotted in Fig. 2(a) as a function of layer thickness. Clearly, for layers exceeding the critical thickness h_c of 1 ML, $\langle L \rangle$ rapidly decreases and converges to $L_\infty = b/\varepsilon_0 = 8.8$ nm where the whole lattice mismatch is accommodated by misfit dislocations. The corresponding relaxed strains $\varepsilon_{\text{rel}} = b/\langle L \rangle$ perfectly agree with *in situ* reflection high-energy electron diffraction measurements.

The excellent agreement of the critical layer thickness and the average dislocation spacings with the equilibrium values predicted by the Matthews-Blakeslee model [7] [$h_{c,\text{MB}} = 1$ ML and solid line in Fig. 2(a)] indicates that strain relaxation is not retarded by kinetic barriers. This implies the operation of a very efficient dislocation nucleation mechanism. Indeed, from STM images recorded at the onset of strain relaxation [Figs. 2(c) and 2(d)], it is found that *all* dislocations are initially introduced by spontaneous nucleation of dislocation half-loops uniformly over the free surface. Once formed, these half-loops rapidly expand and elongate in the lateral direction to form the strain relaxing misfit dislocation segments. Usually, such homogeneous half-loop nucleation is associated with rather high nucleation barriers. Using continuum elasticity theory, the total energy E_{hl} of a semicircular edge dislocation half-loop as function of its radius R is given by [7,8]

$$E_{hl} = \frac{\mu b^2 R}{8(1-\nu)} \ln\left(\frac{2.3R}{\rho}\right) - \pi \mu b R^2 \left(\frac{1+\nu}{1-\nu}\right) \varepsilon_{\parallel}, \tag{1}$$

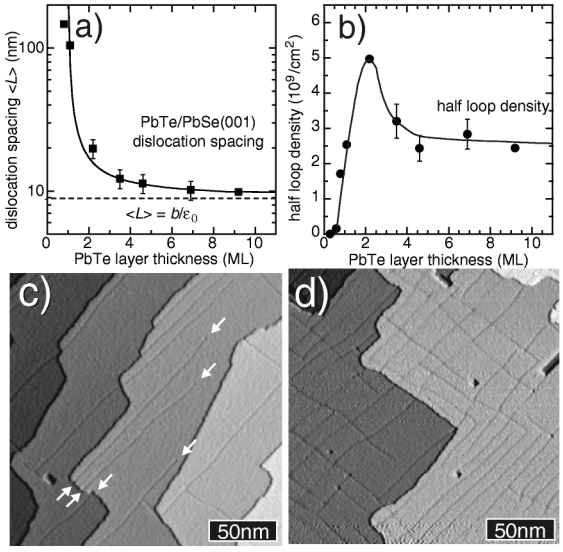

FIG. 2. (a) Average dislocation spacing (■) and (b) density of dislocation (●) half-loops plotted as a function of PbTe layer thickness. Solid line in (a): Theoretically expected equilibrium dislocation spacing. (c) and (d): STM images of PbTe epilayers at 1 and 2 ML coverages, respectively.

where μ and ν are elastic constants, ρ is the dislocation core radius taken as $b/2$, and $\varepsilon_{\parallel}$ is the actual in-plane strain in the layer. In this expression, the first term represents the dislocation self-energy due to the lattice distortions, and the negative second term is the energy gained by strain relaxation. As a half-loop is formed and expands, the total energy first increases to reach a maximum at a certain critical radius R_c, and only thereafter decreases upon further expansion. The energy E_c at this critical radius is the barrier that has to be overcome during the nucleation process. From Eq. (1), it follows that E_c strongly depends on the strain in the layer. In particular, E_c is very large for small misfit systems (typically many eV [7]), such that half-loop nucleation is *kinetically* suppressed. However, with increasing misfit strain, E_c drastically decreases such that an energy of only 800 meV is obtained for the fully strained PbTe/PbSe case. This is well below the threshold energy of 50–88 times kT that is usually considered as the limit for dislocation nucleation [7,8,15].

For a detailed characterization of the nucleation process, we have determined the actual half-loop density as a function of layer thickness using a large number of STM images. The result is shown in Fig. 2(b). Clearly, the nucleation rate is very high at the onset of strain relaxation with a corresponding rapid increase in half-loop density. However, from Eq. (1), with progressing strain relaxation, the nucleation barrier strongly increases and, thus, half-loop nucleation becomes increasingly difficult as growth proceeds. This is exactly the behavior observed in Fig. 2(b), where after the initial increase the half-loop density reaches a maximum at about 2 ML, thereafter decreasing to the final value of 2.5×10^9 cm^{-2}. Thus, beyond 2 ML, strain relaxation mainly proceeds via elongation of existing dislocations rather than by additional half-loop nucleation. At 2 ML the residual strain has already decreased below 2.5%. From Eq. (1), this corresponds to a *tenfold* increase in the nucleation barrier to values greater than 7 eV. This is obviously too large for further half-loop nucleation.

Comparing the STM images recorded at different coverages, obviously a very rapid equilibration of the dislocation spacings occurs during growth. To quantify this effect, we have measured the distribution of misfit dislocation spacings as a function of PbTe coverage. The resulting histograms are shown in Figs. 3(a) to 3(c) for PbTe thicknesses of 2, 4.5, and 9 ML, respectively. For the thin 2 ML layer [Fig. 3(a)], the distribution is very broad with a standard variation σ of $\pm 70\%$ with respect to the average spacing of $\langle L \rangle = 22.8$ nm. However, as growth proceeds, the distribution drastically narrows, reaching a variation of $\pm 20\%$ for the 4.5 ML layer and of only $\pm 12\%$ for the 9 ML layer where $\langle L \rangle$ is only 10 nm. This rapid equilibration process implies a high mobility of the misfit dislocation within the interface as well as a mutual repulsive interaction between neighboring dislocations. The presence of both effects can be already inferred from the STM image of Fig. 1(d), where at each point ($\perp$), where an additional dislocation is introduced in the array, the adjacent

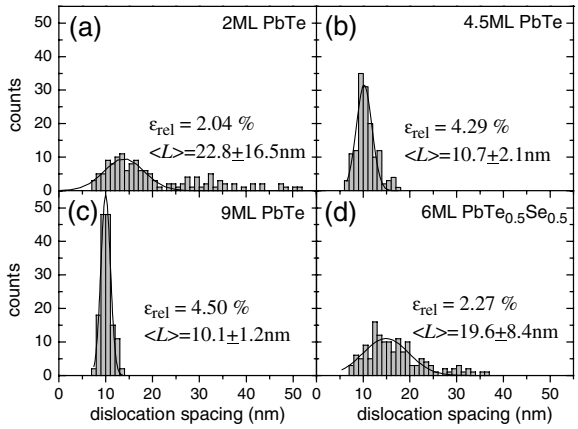

FIG. 3. Histograms of the lateral misfit dislocation spacings for PbTe layers at layer thicknesses of (a) 2 ML, (b) 4.5 ML, and (c) 9 ML, as well as for (d) 6 ML $PbSe_{0.5}Te_{0.5}$ on PbSe (100) with a reduced lattice mismatch of 2.6%. $\varepsilon_{\mathrm{rel}} = b/\langle L \rangle$ is the relaxed strain in the layers.

dislocations effectively rearrange and bend over to reestablish the preferred equilibrium spacing.

Because the Burgers vector is parallel to the interface and because in the lead salt compounds the dislocations are highly mobile within the primary {001} glide planes [16], the misfit dislocations may effectively rearrange within the PbTe/PbSe interface when subjected to internal or external stress sources. Here, the major internal sources are the stress fields around each misfit dislocation. These lead to mutual interactions between dislocations, which depend sensitively on the orientation of their Burgers vectors as well as their positions relative to each other. For pure edge dislocations confined to the layer/substrate interface, the lateral interaction force per unit length F_x experienced by a dislocation at a point x between two neighboring dislocations at $x_{1,2} = \pm L$ can be approximated for $|x| \ll L$ by

$$F_x(x) \cong \frac{\mu b^2}{\pi(1-\nu)} \cos\varphi(1 - 2\sin^2\varphi)\,\frac{x}{L^2}, \qquad (2)$$

where φ is the angle of $\vec{b}$ with respect to the interface, and where surface relaxation effects were neglected. For our case of $\varphi = 0$, this interaction is repulsive, i.e., a dislocation at $|x| > 0$ experiences a net force to the center between the bordering dislocations. This force increases linearly with increasing off-center displacement, resulting in an effective driving force for equilibration of the dislocation spacings. However, if $\vec{b}$ is inclined by 45° to the interface, F_x is zero and even changes sign, i.e., becomes *attractive* for larger inclinations. This is actually *destabilizing* for a regular misfit dislocation arrangement. For $\varphi > 0°$, there is also an additional force component perpendicular to the interface, and the *lateral* dislocation mobility is small due to the required climb processes. For dislocations with *mixed* character, the interaction can be either attractive *or* repulsive depending on the relative orientation of the screw components of $\vec{b}$. This applies, e.g., to the 60° dislocations typical for (001)SiGe or III-V

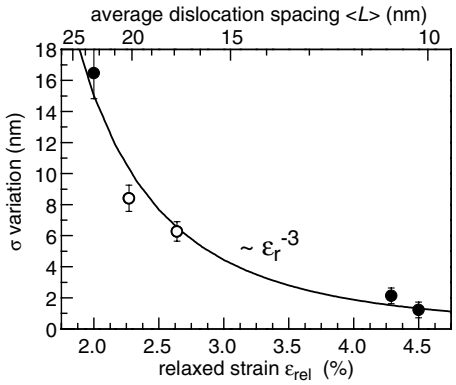

FIG. 4. Dislocation spacing variation σ for different PbTe (●) and $PbSe_{0.5}Te_{0.5}$ (○) thicknesses plotted versus relaxed strain $\varepsilon_{\mathrm{rel}} = b/\langle L \rangle$. Solid line: Power law fit of experimental data.

heterostructures where the interaction F_x is solely determined by the screw component ($\varphi = 45°$). Furthermore, there is an additional elastic interaction between crossing dislocations if their Burgers vectors are *not* perpendicular to each other. This may also influence the dislocation rearrangements.

From Eq. (2), the strength of the interaction scales as $1/L^2$ with decreasing dislocation spacing. Therefore, a more homogeneous arrangement should be formed the smaller the average dislocation spacing, i.e., the larger the relaxed strain $\varepsilon_{\mathrm{rel}}$ in the layer. The dependence of the σ spread of dislocation spacings as a function of $\varepsilon_{\mathrm{rel}}$ is shown in Fig. 4, where we have also included the data from $PbSe_{0.5}Te_{0.5}$ layers (open circles) for which a representative histogram is shown in Fig. 3(d). Clearly, for all samples, the variation in the dislocation spacings drastically decreases with increasing strain relaxation. However, whereas the interaction force in Eq. (2) scales as L^{-2}, the power law fit of the experimental $\sigma(L)$ data (solid line in Fig. 4) yields a scaling exponent of about 3. This deviation is explained by the fact that, for near surface dislocations, the stress fields decay more rapidly as compared to those in bulk material [15], i.e., the interactions between near surface dislocations will depend even stronger on L than predicted by Eq. (2). This underlines the crucial importance of the narrow dislocation spacings for the homogenization process.

For applications of the periodic dislocation array, the strong lateral strain variations caused by the misfit dislocation network have to be considered. For this purpose, we have modeled the surface strain distribution induced by a periodic edge dislocation array based on the work in Ref. [12]. For the 9 ML PbTe layer and 10 nm misfit dislocation spacing, a total in-plane surface strain variation as large as $\Delta\varepsilon_{\parallel} = 3.2\%$ is obtained, which corresponds to an energy variation of 47 meV/surface adatom pair across the array. This is comparable to kT at typical growth temperatures and should therefore be large enough to induce an ordered nucleation of self-organized islands on top of the array. Because of the deformation potentials, the strain variations also modify the local electronic band structure in the layers. Using Ref. [17], $\Delta\varepsilon_{\parallel} = 3.2\%$ translates into a modulation of the PbTe band edges by as much as 120 meV, which leads to a lateral confinement of the free carriers on a length scale of 10 nm.

In conclusion, the dislocation patterning process relies on uniform dislocation nucleation, a strong mutual repulsion, and a high dislocation mobility within the interface. Generally, these criteria are met only in high misfit heteroepitaxial systems because only when (i) homogeneous nucleation is favored over heterogeneous nucleation, (ii) the dislocation interactions are strong due to the narrow dislocation spacings, and (iii) because dislocations with $\vec{b}$ parallel to the interface are preferred over mixed-type dislocations [18] due to the lower nucleation barriers for 90° edge dislocations [7]. On the other hand, since homogeneous dislocation formation is expected only for uniform 2D layers, appropriate growth orientations or surfactants must be used to overcome the strong strain-induced coherent islanding tendency typical for high misfit systems. A particularly important property of the periodic misfit dislocation array is that it minimizes the elastic interaction energies. Thus, it represents the *ideal* lowest energy configuration of strain-relaxed layers in thermodynamic equilibrium. Therefore, significant further improvements in regularity should be obtainable by annealing. This could lead the way to fabrication of novel ordered nanostructures.

This work was supported by the FWF, GME and Academy of Sciences (APART) of Austria.

[1] See, e.g., V. A. Shchukin and D. Bimberg, Rev. Mod. Phys. **71**, 1125 (1999).
[2] D. Leonard *et al.,* Appl. Phys. Lett. **63**, 3203 (1993).
[3] K. Häusler *et al.,* Phys. Rev. B **54**, 4913 (1996).
[4] S. Shiryaev *et al.,* Phys. Rev. Lett. **78**, 503 (1997).
[5] R. Leon *et al.,* Appl. Phys. Lett. **74**, 2301 (1999).
[6] E. Romanov *et al.,* Appl. Phys. Lett. **74**, 2280 (1999).
[7] R. Hull and J. Bean, Crit. Rev. Solid State Mater. Sci. **17**, 507 (1994).
[8] E. A. Fitzgerald *et al.,* J. Vac. Sci. Technol. B **10**, 807 (1992).
[9] G. Springholz *et al.,* Phys. Rev. Lett. **84**, 4669 (2000); Science **282**, 734 (1998).
[10] R. F. Egerton, Surf. Sci. **24**, 647 (1971).
[11] R. Stalder, H. Sirringhaus, N. Onda, and H. von Känel, Appl. Phys. Lett. **59**, 1960 (1991).
[12] G. Springholz, V. Holy, and G. Bauer, Phys. Rev. B **54**, 4500 (1996).
[13] G. Springholz, Appl. Surf. Sci. **112**, 12 (1997).
[14] Similar results were reported, e.g., by L. S. Palatnik and A. I. Fedorenko, J. Cryst. Growth **52**, 917 (1981).
[15] J. P. Hirth and J. Lothe, *Theory of Dislocations* (McGraw-Hill, New York, 1985).
[16] P. Müller *et al.,* Phys. Rev. Lett. **78**, 3007 (1997).
[17] J. Singleton *et al.,* J. Phys. C **19**, 77 (1986).
[18] J. P. C. Chang, T. P. Chin, and J. M. Woodall, Appl. Phys. Lett. **69**, 981 (1996); A. Trampert, E. Tournie, and K. H. Ploog, Appl. Phys. Lett. **66**, 2265 (1995).